Neuron
Article

Presynaptic Regulation of Astroglial Excitatory Neurotransmitter Transporter GLT1

Yongjie Yang,[1] Oguz Gozen,[1] Andrew Watkins,[1] Ileana Lorenzini,[1] Angelo Lepore,[1] Yuanzheng Gao,[1] Svetlana Vidensky,[1] Jean Brennan,[1] David Poulsen,[2] Jeong Won Park,[3] Noo Li Jeon,[3] Michael B. Robinson,[4] and Jeffrey D. Rothstein[1,*]
[1]Department of Neurology and Neuroscience, Johns Hopkins University, Baltimore, MD 21287, USA
[2]Department of Biomedical and Pharmaceutical Sciences, University of Montana, Missoula, MT 59812, USA
[3]Department of Biomedical Engineering, University of California Irvine, Irvine, CA 92697, USA
[4]Children's Hospital of Philadelphia, Department of Pediatrics and Pharmacology, University of Pennsylvania, Philadelphia, PA 19104, USA
*Correspondence: jrothstein@jhmi.edu
DOI 10.1016/j.neuron.2009.02.010

SUMMARY

The neuron-astrocyte synaptic complex is a fundamental operational unit of the nervous system. Astroglia regulate synaptic glutamate, via neurotransmitter transport by GLT1/EAAT2. Astroglial mechanisms underlying this essential neuron-glial communication are not known. We now show that presynaptic terminals regulate astroglial synaptic functions, GLT1/EAAT2, via kappa B-motif binding phosphoprotein (KBBP), the mouse homolog of human heterogeneous nuclear ribonucleoprotein K (hnRNP K), which binds the GLT1/EAAT2 promoter. Neuron-stimulated KBBP is required for GLT1/EAAT2 transcriptional activation and is responsible for astroglial alterations in neural injury. Denervation of neuron-astrocyte signaling by corticospinal tract transection, ricin-induced motor neuron death, or neurodegeneration in amyotrophic lateral sclerosis all result in reduced astroglial KBBP expression and transcriptional dysfunction of astroglial transporter expression. Presynaptic elements dynamically coordinate normal astroglial function and also provide a fundamental signaling mechanism by which altered neuronal function and injury leads to dysregulated astroglia in CNS disease.

INTRODUCTION

The core elements of the central nervous system (CNS) functional unit include presynaptic axons, postsynaptic dendrites, along with the perisynaptic astroglia which ensheathe the vast majority of all synapses. Astroglia play a vital and active role in synaptic transmission (Halassa et al., 2007), by regulating extracellular K^+ concentration, by releasing gliotransmitters, and by modulating glutamate receptor (GluR) activation through glutamate transporter (GluT)-mediated control of synaptic and extra-synaptic glutamate clearance (Huang and Bergles, 2004). The astroglial specific plasma membrane glutamate transporter subtype GLT1 and its human homology, EAAT2 are the dominant functional/physiologically active transporter in the CNS (Danbolt, 2001; Regan et al., 2007; Rothstein et al., 1994b; Tanaka, 1997). GLT1/EAAT2 is typically concentrated in perisynaptic membranes (Chaudhry et al., 1995; Danbolt, 2001). GluTs directly contend with GluRs for glutamate, modulating the intensity and duration of postsynaptic activation and preventing the interference ("spillover" or "spillout") of neighboring synapses (Arnth-Jensen et al., 2002; Huang and Bergles, 2004). Importantly, astroglial GluTs also prevent accumulation of extracellular glutamate and subsequent over-stimulation of GluRs, thus preventing possible excitotoxic neuronal death (Rothstein et al., 1996; Tanaka, 1997). Experimental disruption of this astroglial function is neurotoxic and promotes neurodegeneration (Rothstein et al., 1996). In neurological diseases, the neuron-astroglia synaptic unit is often disrupted, as reflected by severe loss of synaptic astroglial GluTs in postmortem human tissue and rodent models of neurodegeneration (Lauriat et al., 2007; Lievens et al., 2001; Rothstein et al., 1992).

Despite of the importance of astroglial GluTs in synaptic function, the normal molecular regulation of the neuron-astrocyte functional unit is not known. Induction of astroglial GluT expression occurs in parallel with synapse maturation in early postnatal development (Furuta et al., 1997). Multiple in vitro studies of mixed neuron glial cultures suggested that unknown neuronal secreted factors, added glutamate and/or growth factors can induce expression of astroglial glutamate transporters GLT1 and GLAST (Munir et al., 2000; Schlag et al., 1998; Swanson et al., 1997; Zelenaia et al., 2000) or regulate its cytoplasmic clustering (Nakagawa et al., 2008; Zhou and Sutherland, 2004), but downstream molecular mechanisms have not yet explored. In vivo studies demonstrate that alteration of sensory activity by whisker stimulation induces changes in astroglial synaptic coverage and expression levels of astroglial GluTs, suggesting that neuronal activity could be linked to astroglial GluTs genomic regulation (Genoud et al., 2006). With the recent identification of the GLT1/EAAT2 promoter (Su et al., 2003), it became possible to evaluate GluT transcriptional regulation and the contribution of synaptic elements to this astrocytic perisynaptic protein. In this study, we have identified the transcriptional mechanisms that underlie normal neuronal/synaptic regulation of astroglial GLT1/EAAT2 and how in vivo disruption of this astroglial pathway may be common to subacute and chronic neuronal disease.

RESULTS

Axons Are Sufficient and Necessary for Transcriptional Activation of Astroglial GLT1

A microfluidic culture platform (MCP; Park et al., 2006; Figure 1A) was used to develop a neuron and astrocyte coculture system in which only axons penetrate and establish contact with astrocytes, thereby providing a system to study the role of neuronal processes on GLT1 activation at a single axon/astrocyte resolution. High-density neurons (1–3 × 10^6/ml) were first plated on the right side of the MCP. GDNF (10 ng/ml) was added to the left side of the MCP to stimulate axon outgrowth 24 hr after seeding of neurons. Extensive neuronal processes grew through channels connecting both sides of MCP 3–5 days after adding GDNF (Figures 1A and 1B). A representative magnified image of axon and astrocyte is shown in Figure 1B. More than 90% of neuronal processes growing through the channels are axons, as confirmed by unique growth cone morphology, immunoreactivity for the growth cone marker 2G13 (Figure 1A), and for synapsin-I (see Figure S1A available online) and immunonegative for MAP2 (data not shown). The solution exchange between both sides of the MCP is minimal (Park et al., 2006), as no DiI and DiO double-labeled astrocytes were observed in each side of the MCP (Figure S1B) nor was there leakage of ^{3}H-glutamate between chambers (data not shown). To establish neuron astrocyte coculture in the MCP, GDNF was removed when neuronal processes were still inside the connecting channel, and astrocytes were plated into the left chamber. As shown in Figures 1B and 1C, axon bundles, visualized by βIII-tubulin staining, passed through the channel, entering the astrocyte side of MCP. Intensity of GLT1 immunostaining (10990 ± 791, arbitrary units) in astrocytes with the presence of axons was significantly increased 230% (Figure 1D) compared to that in astrocytes alone chamber (4781 ± 385), indicating that axons are sufficient to induce GLT1 activation. Axonal activation of GLT1 expression is apparently axon number/length dependent, as the intensity of GLT1 staining (12350 ± 732) in platforms with more axons (indicated by the total length, 7,500–18,889 μm/mm^2) is significantly higher than that (7409 ± 872) in platforms with fewer axons (3700–7500 μm/mm^2; Figures 1C and 1D). In this model paradigm, the vast majority of GLT1 activation was only seen with astrocytes contacted by axons (white arrows in Figures 1B and 1C). Highest GLT1 intensity was found in all astrocytes with axon contact. Only occasional astrocytes, with no obvious direct axon/terminal contacts, were also GLT1 activated (yellow arrow in Figure 1C). Subsequent treatment of cultured astrocytes with differential neuronal components, i.e., neuronal supernatant (NS), neuronal membrane (NM), or neuron conditional medium (NCM) were all sufficient to increase GLT1 expression, to a similar level (Figures S1C and S1D). These results would suggest that presynaptic interactions with astroglia via direct contact might activate transcriptional pathways in astroglia.

To study molecular modulation of astroglial synaptic-relevant pathways, we utilized BAC GLT1 eGFP promoter reporter mice (Regan et al., 2007), which allow spatial and temporal in situ monitoring of single astrocyte GLT1 promoter activity by fluorescence reporter intensity. The expression of the reporter correlates with endogenous GLT1 promoter activation, protein expression, and functional activity (Regan et al., 2007). To monitor dynamic changes of the GLT1 promoter to axon stimulation, astrocytes derived from this mouse were added on the left side of MCP after culturing neurons for 3–5 days, prior to entry of axons into the astroglial chamber. Time-lapse images were collected from 24 to 112 hr after coculture (Figure 1E). Intensity of eGFP fluorescence, the indicator of GLT1 genomic promoter activity, in single astrocytes, was detected and represented by pseudocolor (Figure 1E). In the absence of axons, no GLT1 appreciable gene activation was observed. Dramatic increase of eGFP intensity was observed (from 2846 ± 682 to 10860 ± 941) within 48 hr after axons approach and/or make contact with the astroglia (24–68 hr; Figure 1G). The dependence of the axon-astrocyte interaction was validated by the decrease in astrocytic eGFP expression (68–112 hr), following kainate-induced (200 μM; added to neuronal side) neural injury and subsequent axonal degeneration (Figures 1E and 1F). In contrast, eGFP intensity from MCP without application of kainite only decreased slightly from 68 to 112 hr (Figure 1G). Axon-dependent eGFP intensity changes, quantified from these time-lapse images, clearly indicate that axons induced transcriptional activation of GLT1. GLT1 mRNA levels were also increased after directly adding neurons to astrocyte cultures (Figure S1E), providing additional evidence that synaptic interaction with astroglia induces transcription activation of GLT1.

We further investigated whether glutamate receptor (GluR)-mediated neuron-astroglial signaling is involved in neuron-dependent GLT1 activation. P8 rat spinal cord organotypic slice cultures, a system faithfully mimicking the in vivo environment (Rothstein et al., 1993), were used to investigate altered neuron-astrocyte communication on GLT1 activation. As spinal cord slices are usually 350 μm in thickness, relatively higher concentrations of pharmacological inhibitors were used in experiments. GLT1 expression levels in slice cultures were reduced in a dose-dependent manner following tetrodotoxin (TTX) treatment (Figures 2A and 2B), suggesting that Na^+ channel-mediated synaptic transmission facilitates GLT1 activation in astrocytes. In addition, treatment of slice cultures with ionotropic or metabotropic GluR antagonist cocktails also resulted in a dose-dependent decrease of GLT1 expression (Figures 2A, 2B, 2E, and 2F). Inhibition of astroglial iGluRs in astrocytes in MCP also leads to decrease of axon-induced GLT1 expression (Figures S2A and S2B). Subsequent treatment of slices with individual glutamate receptor antagonists revealed that AMPA (antagonist CNQX) and mGluR 1/5 (antagonist m196) are involved in the neuron-dependent GLT1 activation (Figures 2C, 2D, 2G, and 2H). NMDA antagonist MK801 had little effect, although high-dose APV was inhibitory (Figures 2C and 2D). Overall, mGluR1/5 antagonists alone or in combination appeared to have the greatest effect on GLT1 expression in the slice culture paradigm (Figures 2E, 2F, 2G, and 2H). GluRs are expressed on pre- and postsynaptic neurons as well as astrocytes, thus, inhibition of GluRs results in inhibition of synaptic transmission from neuron-to-neuron and neuron-to-astrocyte. The block of GLT1 activation by inhibition of neurotransmitter release (TTX) and by the GluR receptor antagonists suggests that synaptic activity is a strong component of presynaptic-based activation of astroglial GLT1.

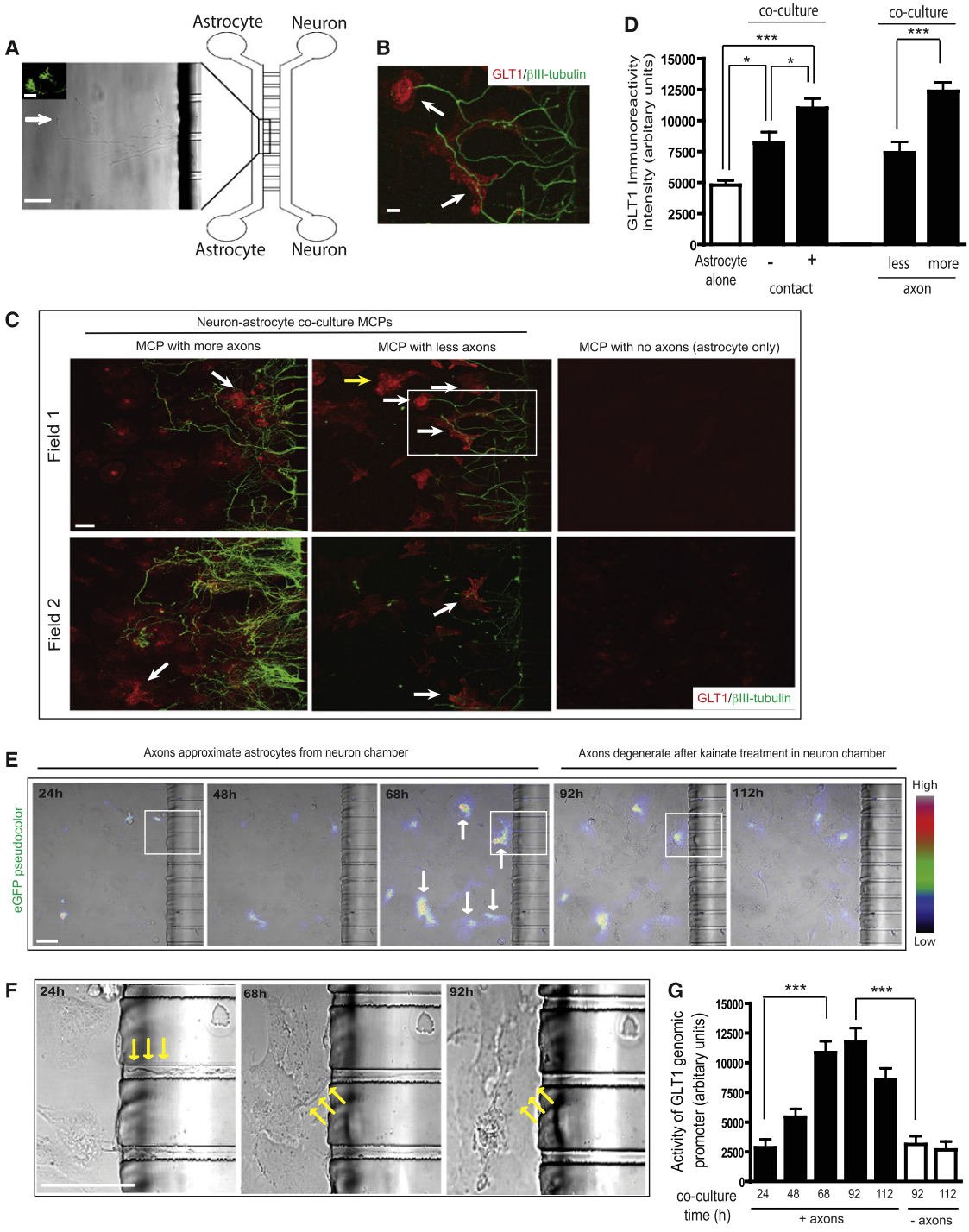

Figure 1. Axon-Dependent Transcriptional Activation of GLT1 Promoter and GLT1 Protein Expression on a Microfluidic Culture Platform (MCP)

(A) Diagram of an astrocyte neuron coculture system using a microfluidic culture platform (MCP). Growth cone is stained with 2G13 antibody. Scale bar, 20 μm (insert scale bar, 10 μm).

(B) Magnified view of the interaction between axons and astrocytes. Astrocytes were stained with GLT1 and axons were stained with βIII-tubulin antibody. Scale bar, 50 μm.

(C) Axons are sufficient to induce GLT1 upregulation in cultured astrocytes on MCP. Astrocytes were stained with GLT1 and axons were stained with βIII-tubulin antibody. White arrow: astrocyte with axon contact; yellow arrow; astrocyte without axon contact; Representative two fields were shown from each group. Scale bar, 50 μm.

Previous in vitro preparations from mixed neuron-glial cultures had suggested that neuron conditioned medium can directly activate the expression of GLT1 (Gegelashvili et al., 1997; Schlag et al., 1998; Swanson et al., 1997) and that soluble factors may be secreted from neurons to stimulate the expression of astroglial glutamate transporter. Glutamate has long been speculated as one of the soluble factors that increase GLT1 expression, but direct exposure of high concentration of glutamate in vitro to astrocyte cultures fails to increase GLT1 expression but does alter its cytoplasmic clustering (Nakagawa et al., 2008; Zhou and Sutherland, 2004). In fact, elevated levels of glutamate are closely associated with loss of EAAT2 in chronic neurological injuries including ALS, Huntington's disease, and multiple sclerosis, suggesting that other released factors or altered membrane contact may play more important roles in mediating axon-induced GLT1 activation. For example, axon membrane contact can be a potent regulator of developmental astroglial Notch signaling (Eiraku et al., 2005). By using this isolated neuron astrocyte coculture system, our results prove that astroglial activation is neuron dependant and that presynaptic interaction with astroglia including both secretion and direct membrane contact, transcriptionally activate astroglial GLT1.

Recruitment of Kappa-B Motif-Binding Phosphoprotein (KBBP) to the Promoter Is Required for GLT1 Transcriptional Activation

To evaluate how neurons regulate astroglial GLT1/EAAT2, we cloned a 2.5 kb upstream promoter of human EAAT2 that shares high sequence homology (>70%) with GLT1 promoter from multiple species (Rothstein et al., 2005). To test whether this 2.5 kb promoter behaves similarly as full-length (15 kb) GLT1 genomic promoter in rodent astrocytes, a DsRed EAAT2 promoter reporter (2.5 kb; Figure 3A) was transfected into astrocyte cultures derived from BAC GLT1 eGFP transgenic mice (Regan et al., 2007). After transfection, newly prepared cortical neurons were plated on transfected astrocytes. As shown in Figure 3A, the presence of neurons markedly induced the expression of both DsRed and eGFP reporters in the same astrocyte, indicating that the 2.5kb promoter is functional in a rodent astrocyte environment and contains conserved *cis*-elements sufficient for neuron-derived activation signals.

To identify the major promoter regions responsible for neuron-dependent activation, luciferase promoter reporters were generated by serial deletion of the 2.5 kb sequence and electroporated into P2 mouse primary astrocyte cultures. Sequence deletion from −921 to −279 (pGL958 versus pGL316 in Figure 3B) sharply reduced both basal and neuron-dependent promoter activity (Figures 3B and 3C), with the most significant drop of activity from pGL958 to pGL557, indicating that the sequence between −921 to −520 contains primary elements for neuron-dependent GLT1 promoter activation. Multiple highly conserved transcription factor binding sites are present in the region from −921 to −520 by sequence analysis. Site-directed mutagenesis of pGL958 generated multiple mutant luciferase promoter reporters, which were examined in astrocyte cultures (Figure 3D). The 958bp mutant 2 exhibited the greatest reduction in luciferase activity without altering cotransfected β-galactosidase activity, suggesting that the sequence mutated from −688 to −679 GGGTGGGTGT is essential for GLT1 promoter activity. Sequence alignment across ten species characterized GGGTGGGTGT as an evolutionally conserved site among mammals (Figure S3A). Notably, mutations of putative NF-κB binding sites within this promoter region had no dramatic influence on neuron stimulated promoter activation (data not shown).

The requirement of nucleotides −688 to −679 for GLT1 promoter activity was further tested in vivo. GLT1 mRNA transcription is strongly induced during early postnatal development in rodent brain (Schmitt et al., 1996; Sutherland et al., 1996), providing an in vivo model to test the GLT1 promoter activation. A DsRed reporter driven by the wild-type 958bp or 958bp mutant 2 EAAT2 promoters was delivered to brain of young mice using an adeno-associated virus (AAV) vector to examine in vivo reporter activation. AAV particles carrying the EAAT2 promoter DsRed expression cassette were injected into the lateral cerebral ventricle of P0 pups of BAC GLT1 eGFP transgenic mice (Broekman et al., 2006). As shown in Figure 3E, confocal analysis of coronal brain sections of mice, 3 weeks after injection with 958bp-WT-DsRed containing AAV revealed expression of the DsRed reporter in astrocytes that also express eGFP reporter. However, no expression of DsRed was found from brain sections of mice injected with 958 bp mutant 2-DsRed containing AAV. Expression of the DsRed was also seen in nearby neurons for both AAV viruses (data not shown), suggesting that both viruses are effective in driving the DsRed reporter expression in vivo. The inability of 958 bp mutant 2 promoter to drive DsRed reporter expression in astrocytes in vivo confirmed the in vitro results that the sequence from −688 to −679, GGGTGGGTGT, is essential for neuron-dependant EAAT2 promoter activity.

The nuclear factors recruited to the GGGTGGGTGT sequence, were identified by performing a gel shift assay with nuclear extracts prepared from mouse cortex at developmental time points prior to GLT1 promoter activation (P2) and after strong promoter activation (P21). Wild-type and mutant oligos (45-mer) that only differ in the GGGTGGGTGT were synthesized and labeled with biotin. As shown in Figure 3F, increased specific binding with labeled WT oligo was found from P2 to P21 mice when the GLT1 promoter was strongly activated. The addition

(D) Quantitative analysis of axon-induced GLT1 expression (5–10 astrocytes per field, 2–3 field/MCP from total 5–7 MCPs).
(E) Time-lapse recording of astrocytic eGFP (from BAC GLT1 eGFP mice) fluorescence and outgrowth of axons within MCP. Confocal images were collected 24 to 112 hr after coculture. eGFP fluorescence intensity in astrocyte using pseudocolor represention (Image J). Kainate (200 μM) was added to the right side of MCP after taking images at 68 hr to induce neural injury and axon degeneration. The exchange of solution between chambers is very minimal. Direct treatment of kainite (200 μM) to astrocyte did not change GLT1 expression and astrocyte viability. Scale bar, 50 μm.
(F) Magnified view of axon and astrocyte interaction in MCP. Examples of axons (yellow arrow) that extend through MCP channels (24–68 hr) and axonal degeneration after kainite treatment (68–92 hr). Scale bar, 50 μm.
(G) Quantitative analysis of axon-dependent change of eGFP fluorescence intensity from time-lapse images (5–8 astrocytes per field, 2–3 fields/MCP from total 3–5 MCPs (*$p < 0.05$, ***$p < 0.001$, mean ± SEM, one-way ANOVA and Bonferroni post hoc analysis).

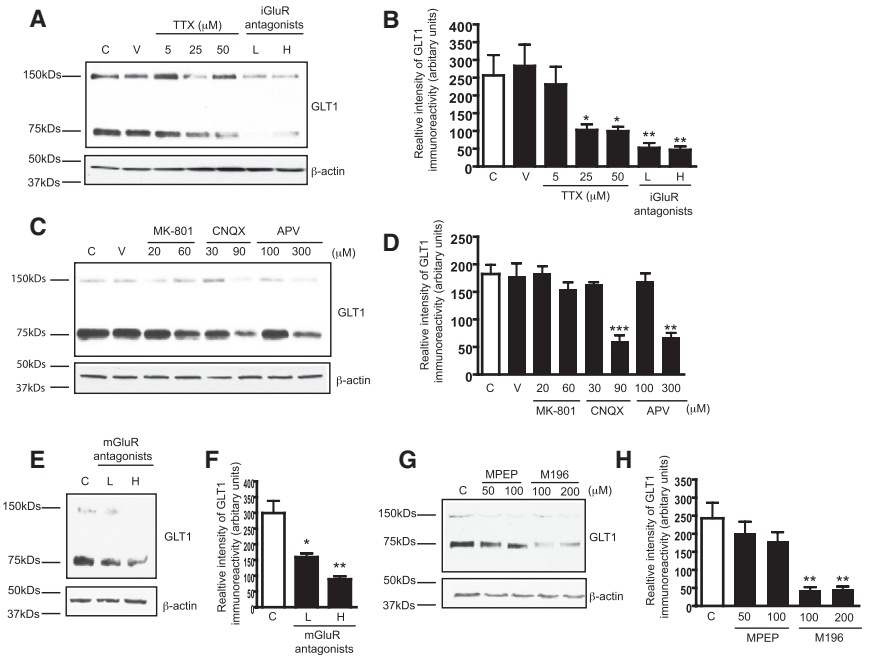

Figure 2. Glutamate Receptors Are Involved in Neuron-Dependent GLT1 Expression

(A) Dose-dependent reduction of GLT1 expression levels induced by TTX (5–50 μM) and iGluR antagonist cocktail treatment (7 days) in rat organotypic spinal cord slice cultures. L: low dose of cocktail (20 μM MK801 + 30 μM CNQX + 100 μM APV); H: high dose of cocktail (60 μM MK801 + 90 μM CNQX + 300 μM APV).

(B) Densitometric analyses of GLT1 immunoreactivity from immunoblot following seven day TTX or iGluR antagonist cocktail treatment (n = 3).

(C) Effect of individual iGluR antagonists on neuron-dependent GLT1 expression. Rat spinal cord cultures were treated with individual iGluR antagonist for 7 days.

(D) Densitometric analyses of GLT1 immunoreactivity from immunoblot with individual iGluR antagonist (n = 3).

(E) Dose-dependent reduction of GLT1 expression levels induced by mGluR antagonist cocktail treatment (7 days) in rat spinal cord slice cultures. L: low dose of cocktail (100 μM M196 + 50 μM MPEP); H: high dose of cocktail (200 μM M196 + 100 μM MPEP).

(F) Densitometric analyses of GLT1 immunoreactivity from immunoblot with mGluR antagonists cocktail treatment (n = 3).

(G) Effect of individual mGluR antagonists on neuron-dependent GLT1 expression. Rat spinal cord slice cultures were treated with individual mGluR antagonists for 7 days.

(H) Densitometric analyses of GLT1 immunoreactivity from immunoblot with individual mGluR antagonists (n = 3). All the immunoblots were quantified in Quantity One software and plotted in PRISM (***p < 0.001, **p < 0.01, *p < 0.05, error bars represent SEM, one-way ANOVA and Bonferroni test was used).

of extraunlabeled WT oligo completely abolished the binding, suggesting that the binding is specific to this oligo. On the other hand, no specific binding with labeled mutant (MT) oligo was found, indicating the change of core sequence from GGGT GGGTGT to AAATGCCACT abolished the recruitment of specific nuclear proteins to this *cis*-element during GLT1 promoter activation. In addition, no other binding with labeled MT oligo was observed, suggesting that the replacement of GGGTGGGTGT with AAATGCCACT does not introduce nonspecific binding with other nuclear proteins. This direct biochemical evidence of gel shift result, along with the genetic analysis in Figures 3D and 3E, demonstrates that the recruitment of nuclear factors to GGGTGGGTGT is essential for neuron-stimulated GLT1 promoter activity.

To identify the actual transcription factor binding to GLT1 regulatory site GGGTGGGTGT, nuclear extracts were affinity purified with the same oligos used in gel shift analysis. After purification, proteins bound to the WT or MT oligos were resolved on 4%–12% PAGE gel and visualized by silver staining. A specific band with molecular weight between 50 to 75 kDa was only found with labeled WT oligo but not with MT oligo (Figure 3G), confirming the results from gel shift analysis. Subsequent trypsin digestion and LC/MS/MS analysis of digested peptides (Figure 3H) revealed a nuclear protein, kappa-B motif-binding phosphoprotein (KBBP, gi|1083569), specifically binds to WT oligo.

KBBP was first identified in a T lymphoma cell line that binds to kappa B enhancer element (GGGGACTTTCC) (Ostrowski et al., 1994). It is almost 100% homologous with human heterogeneous nuclear ribonucleoprotein K (hnRNP K) protein (Ostrowski et al., 1994). HnRNP K protein plays diverse roles in transcription, RNA splicing, and signal transduction through its interaction with many protein partners, including protein kinases, transcriptional factors, and DNA/RNA (Bomsztyk et al., 2004). Notably, although the original kappa B enhancer element GGGGACT TTCC share partial homology with the KBBP binding sequence GGGTGGGTGT on GLT1 promoter, it is sufficient to compete out GGGTGGGTGT induced specific binding with KBBP in a dose-dependent manner (Figure S3B). In addition, further mutation of *GGG* to AAA on KBBP binding sequence *GGG*TGGGTGT also abolished GLT1 promoter activity (Figure S3C), suggesting that these nucleotides are critical for KBBP binding and GLT1 promoter activity. As the mouse homolog of human hnRNP K, KBBP protein may also participate in transcription or RNA splicing. Expression of KBBP in astrocytes in vivo was first examined by using an antibody against human hnRNP K. Cortical immunoreactivity for KBBP in both P2 and P21 BAC GLT1 eGFP mice shows neuronal and astroglial immunolocalization. Notably, KBBP expression was barely detectable in P2 astrocytes and dramatically increased in astroglia from P2 to P21, which is identical to the very large increase in astroglial GLT1 promoter activity (indicated by eGFP reporter intensity) in the same astroglia (Figure 4A). The significant correlation between increased expression of astroglial KBBP and GLT1 promoter/protein (Figure 4B) during early postnatal development suggests that KBBP may play an important role in transcriptional regulation of GLT1. Interestingly, KBBP expression in cultured astrocytes was also induced by neurons, coupled to the increase of GLT1 (Figure 4C); the coupled increases of KBBP and GLT1

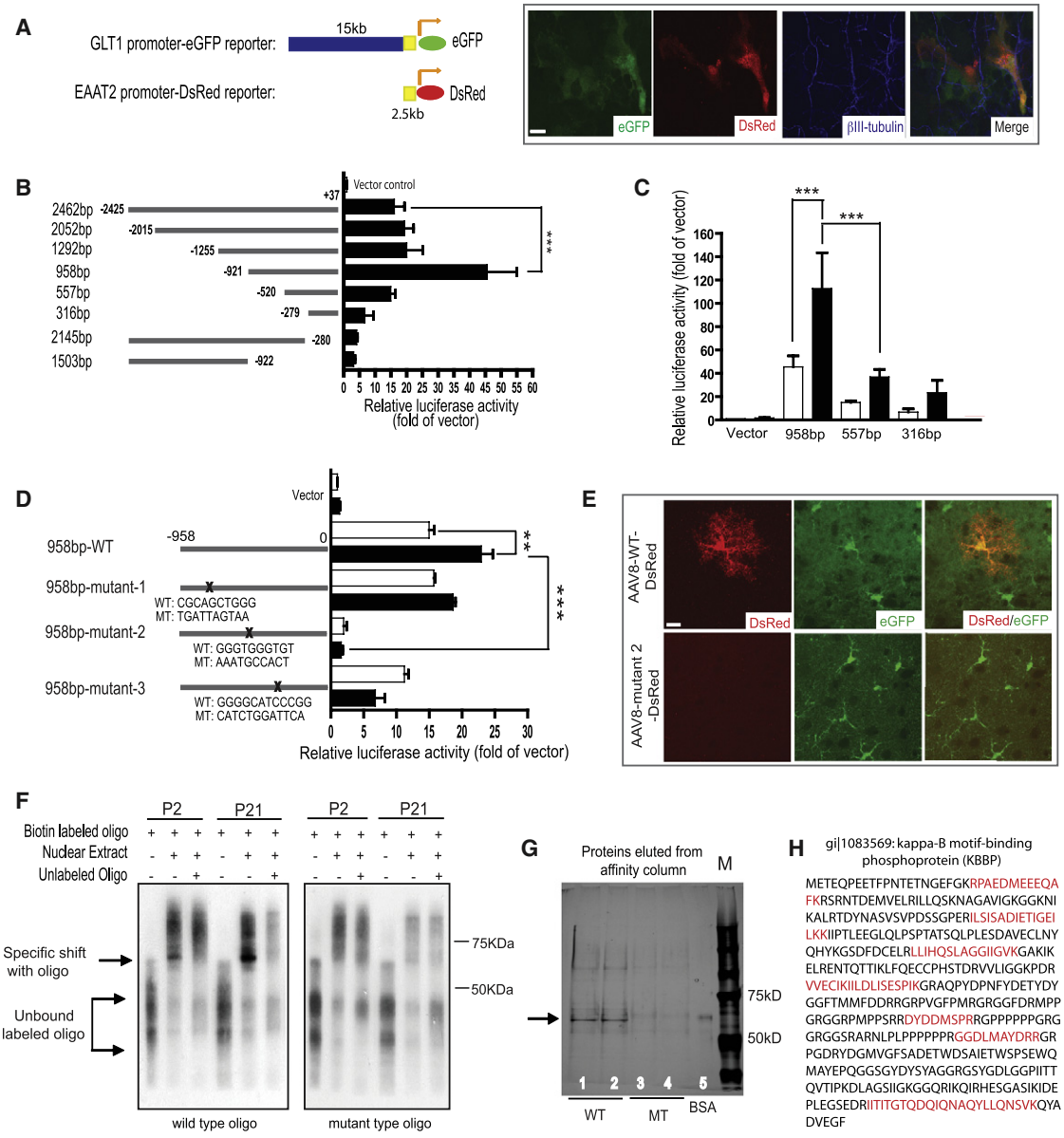

Figure 3. Recruitment of Kappa B-Motif Binding Phosphoprotein (KBBP) to GLT1 Promoter Is Required for Its Activation

(A) A 2.5 kb of human EAAT2 promoter is sufficient for neuronal stimulation in mouse astrocyte environment. The EAAT2 2.5 kb promoter-DsRed reporter and GLT1 genomic promoter-eGFP reporter were both activated in astrocytes following coculture with neurons identified by βIII-tubulin immunostaining.

(B) Identification of the regions essential for the basal activity of human EAAT2 promoter by serial deletion of human EAAT2 promoter (n = 5–7). ***$p < 0.001$; mean ± SEM.

(C) Promoter sequence from −958 bp to −557 bp is mainly responsible for neuron-dependent GLT1 promoter activation in primary astrocytes (n = 4–8). □ = astrocytes alone; ■ = astrocytes and neurons. ***$p < 0.001$; mean ± SEM.

(D) Mutagenesis of GGGTGGGTGT from −688 bp to −679 bp almost completely abolished basal and neuron-dependent GLT1 promoter activity in vitro (n = 6–8). For luciferase assay, luciferase promoter reporters were first electroporated into cultured astrocytes and then freshly prepared neurons were plated on the top of transfected astrocytes. β-galactosidase was cotransfected for normalization. ***$p < 0.001$, **$p < 0.01$, one-way ANOVA and Bonferroni test was used.

(E) Mutagenesis of GGGTGGGTGT from −688 bp to −679 bp abolished GLT1 promoter activation (indicated by DsRed reporter expression) in astrocyte in vivo during early postnatal development. Astrocytes were identified by positive eGFP expression (20–30 astrocytes examined per serial section/mouse for total four mice each).

(F) Mutagenesis of *cis*-element GGGTGGGTGT abolished its specific binding to nuclear factors during GLT1 promoter activation in early postnatal development.

(G) Affinity purification by using wild-type oligo GGGTGGGTGT but not the mutant oligo found unique nuclear protein from P21 mice cortex nuclear extracts.

(H) Trypsin digestion and LC/MS/MS identified Kappa B-motif binding phosphoprotein (KBBP) that specifically binds to GGGTGGGTGT. The red-colored amino acid sequences are small peptide sequences identified from LC/MS/MS that also match with KBBP sequence in NCBI.

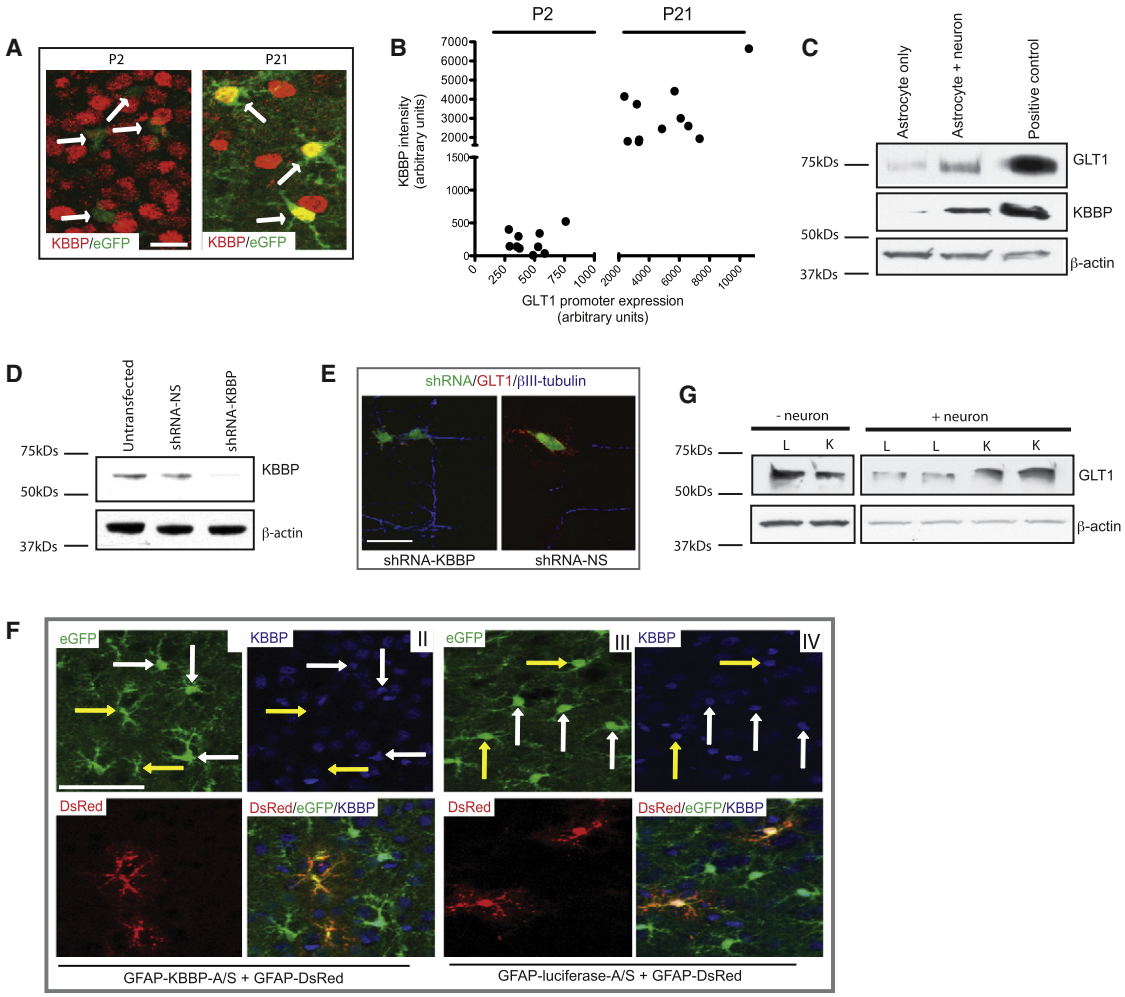

Figure 4. KBBP Is Essential and Sufficient for Neuron-Dependent Transactivation of GLT1

(A) Expression of KBBP protein in astroglia in vivo. KBBP protein expression was minimal in P2 astroglia (BAC GLT1 eGFP reporter, white arrows) and was markedly induced in cortical astrocytes during early postnatal development, along with astroglial BAC-GLT1 eGFP expression (white arrows). Scale bar, 10 μm.

(B) Quantitative correlation of KBBP expression levels and GLT1 promoter activity in astroglia during early postnatal development. Positive linear relationship of KBBP expression levels and eGFP intensity was found. The KBBP immunoreactivity and eGFP fluorescence intensity was quantified in Image J (20 astrocytes examined per serial section/mouse for total 4 mice).

(C) KBBP expression in astrocytes is induced by the presence of neuron. Neurons and astrocytes were cocultured for 1 week before sample collected. Positive control: mice brain lysate.

(D) Development of shRNA that specifically silences KBBP expression. shRNA against KBBP results in over 90% less of KBBP expression in 3T3 NIH cells.

(E) Silencing of KBBP expression by shRNA reduced GLT1 expression in astrocyte on neuron-astrocyte coculture MCP. shRNA-expressing astrocytes were identified by coexpressed eGFP from shRNA construct. GLT1 expression and neuronal processes were visualized by GLT1 or βIII-tubulin immunostaining, respectively. Scale bar, 20 μm.

(F) AAV mediated expression of KBBP antisense in vivo reduced GLT1 promoter activity during early postnatal development. AAV8-GFAP-KBBP-A/S and AAV8-GFAP-DsRed particles were coinjected into cerebral lateral ventricle of P0 pups of BAC GLT1 eGFP transgenic mice. AAV8-GFAP-luciferase-A/S serves as antisense control for AAV8-GFAP-KBBP-A/S. Antisense expressing astrocytes were identified by DsRed reporter expression (20–30 astrocytes examined per serial section/mouse for total 4 mice each). Scale bar, 50 μm (one-way ANOVA with Bonferroni post hoc analysis, $^{**}p < 0.01$, $^{***}p < 0.001$; mean ± SEM).

(G) Overexpression of KBBP in astrocytes increases GLT1 expression with the presence of neurons. L: luciferase overexpression; K: KBBP overexpression. Neurons were plated on transfected astrocyte cultures 2 days posttransfection and kept for 1 week.

are consistent with the same changes in astrocytes observed in vivo.

Small interference RNA (siRNA) specifically against KBBP was developed that effectively reduced KBBP expression level to 10% of that in control (Figure 4D; Moumen et al., 2005), which results in significantly reduced GLT1 expression in astrocytes on neuron-astrocyte coculture MCP (Figure 4E). We further tested whether a decrease of KBBP expression in astrocytes also reduces GLT1 promoter activity in vivo. To selectively silence astroglial KBBP, AAV particles that carried an expression cassette with the KBBP gene in the antisense orientation driven by the GFAP promoter, along with AAV particles that carried

a DsRed reporter expression cassette driven by the same promoter, were intraventricularly injected into new born (P0) BAC GLT1 eGFP transgenic mice. AAV particles carrying luciferase in the antisense orientation served as a control. KBBP antisense was highly effective at silencing KBBP expression in cultured astrocytes (Figure S4C). As shown in Figure 4F, KBBP antisense, but not luciferase antisense, effectively silenced KBBP expression in vivo. GLT1 promoter activity in KBBP antisense-expressing astrocytes, identified by DsRed, was significantly reduced as indicated by reduced eGFP intensity (Figure 4F, I and II, shown by yellow arrow) compared to that in untransduced astrocytes (shown by white arrow) while GLT1 promoter activity in luciferase expressing astrocytes was unaltered (Figure 4F, III and IV, shown in yellow arrow). In aggregate, the loss-of-function analysis of KBBP by RNAi and antisense in astrocytes, along with the promoter mutagenesis analysis, indicate that recruitment of KBBP to the GLT1 promoter is required for GLT1 transcriptional activation in vivo.

We next determined if overexpression of KBBP could concomitantly alter GLT1 expression in astrocyte cultures. KBBP and luciferase overexpression constructs were prepared and electroporated into cultured astrocytes. As shown in Figure 4G, overexpression of KBBP, but not luciferase, was sufficient to increase GLT1 expression in the presence of neurons, though overexpression of KBBP itself was not sufficient to induce the GLT1 expression. In addition, direct treatment of cultured astrocytes with DHPG (50 μM), the selective agonist for mGluR 1/5, increases both GLT1 and KBBP mRNA levels (Figures S4A and S4B), indicating that mGluR 1/5 may play more dominant role in neuron-dependent GLT1 upregulation. Although direct treatment of physiological GluR agonist glutamate failed to increase the GLT1 expression, this could be due to the quick uptake of extracellular glutamate by GLAST in cultured astrocytes. These results are consistent with our observations that astroglial KBBP and GLT1 are expressed in parallel in vivo during early postnatal and synaptic maturation. This hints that the maturation of synapse might influence astroglial gene activation and expression of GLT1. Conversely, an alteration of this pathway due to the loss of presynaptic influence of neurons on astrocytes could be an important event linking neural injury to astroglial synaptic function.

In Vivo Neuron/Axon Denervation Leads to GLT1 Transcriptional Dysregulation through Reduction of KBBP Expression

In order to evaluate the in vivo effect of altered synaptic coupling of neurons to astroglia, we investigated the alterations of astroglial GLT1 gene activation and regulation by KBBP in response to synaptic disruption by using several in vivo models including acute axon denervation induced by corticospinal tract lesion, ricin-induced acute motor neuron degeneration and the chronic neurodegeneration ALS mouse model employing SOD1 G93A mice.

Corticospinal Tract Transection

Corticospinal tracts originating from glutamatergic upper motor neurons possess excitatory presynaptic terminals on spinal cord interneurons and lower motor neurons that are modulated by perisynaptic astroglial GluTs. This pathway allows direct in vivo assessment of astroglial transporter expression in response to the loss of axonal signals induced by spinal cord transection. Thoracic cord (segment 9) transection was performed three weeks after mice received bilateral injection of Fluororuby (FR) into motor cortex to label corticospinal tracts by anterograde FR transport. One week after transection, thin horizontal sections of spinal cord were prepared and FR signals were examined to assess axon degeneration. Above the surgical lesion, abundant FR labeled axons, typical for corticospinal tract innervation, were found bilaterally in spinal cord white matter, projecting to gray matter neurons at each segment (Figure 5A, I). FR-labeled neurons were also observed in gray matter (Figure 5A, II). In contrast, FR signals (including labeled axons and gray matter neurons) were reduced in the cord well below the lesion site in lumbar spinal cord (Figure 5A, III). Quantitative analysis revealed that more than 70% of FR labeled corticospinal axons in lumbar cord were depleted as early as 7 days following spinal transection (Figure 5A). GLT1 protein expression in lumbar cord of lesioned mice was markedly reduced compared to that of control mice (Figure 5B). A pronounced loss of GLT1 immunostaining was also observed in coronal sections of lesioned lumbar cords from BAC GLT1 eGFP mice. GLT1 promoter activity, as reflected by eGFP fluorescence intensity in coronal sections of lumbar cord of lesioned BAC GLT1 eGFP mice, was focally reduced (Figures 5C and 5D) in single astrocytes. These sharp astroglial changes were localized to regions with diminished synaptic terminals, as identified by the loss of presynaptic terminal marker vesicle glutamate transporter 1 (VGluT1), VGluT2 (Figure S5A) and preservation of postsynaptic marker PSD95.

Overall, the loss of KBBP in individual astroglia (Figure 5E, yellow arrow) correlated with a decrease in GLT1 promoter-reporter eGFP intensity in same cells in lesioned lumbar cord (Figure 5E), along with loss of GLT1 protein (Figure 5B). The astroglial changes all followed the loss of presynaptic terminals. These in vivo studies demonstrate that presynaptic terminals act to maintain astroglial KBBP expression, which in turn activates GLT1 expression. Furthermore, these data provide a pathway by which abnormal axon/presynaptic signaling can alter astroglial synaptic integrity.

Neurotoxin Lesion

Neurodegeneration could alter the physiologic axon/astrocyte communication required for astroglial synaptic maintenance. The neurotoxin ricin, an extremely potent protein synthesis inhibitor, has been well established as a model for selectively lesioning discrete populations of motor neurons, through retrograde transport. In order to examine the response of individual astroglia in vivo, to the focal loss of spinal motor neurons, and their recurrent axon collaterals, we injected selected peripheral nerves with the toxin. Femoral nerves (originated from lumbar cord 2–4) of BAC GLT1 eGFP mice were dipped into fluororuby (FR) solution or mixture of ricin and FR solution unilaterally so that the change of GLT1 promoter activity in response to motor neuron death could be directly assessed at the same segment. As shown in Figure 6A, motor neurons were clearly labeled with FR in the control side of L2–L4 cord sections but not in the ricin injected side due to degeneration of motor neurons 1 week following injection (magnified view in Figure 6C). Mice received unilateral

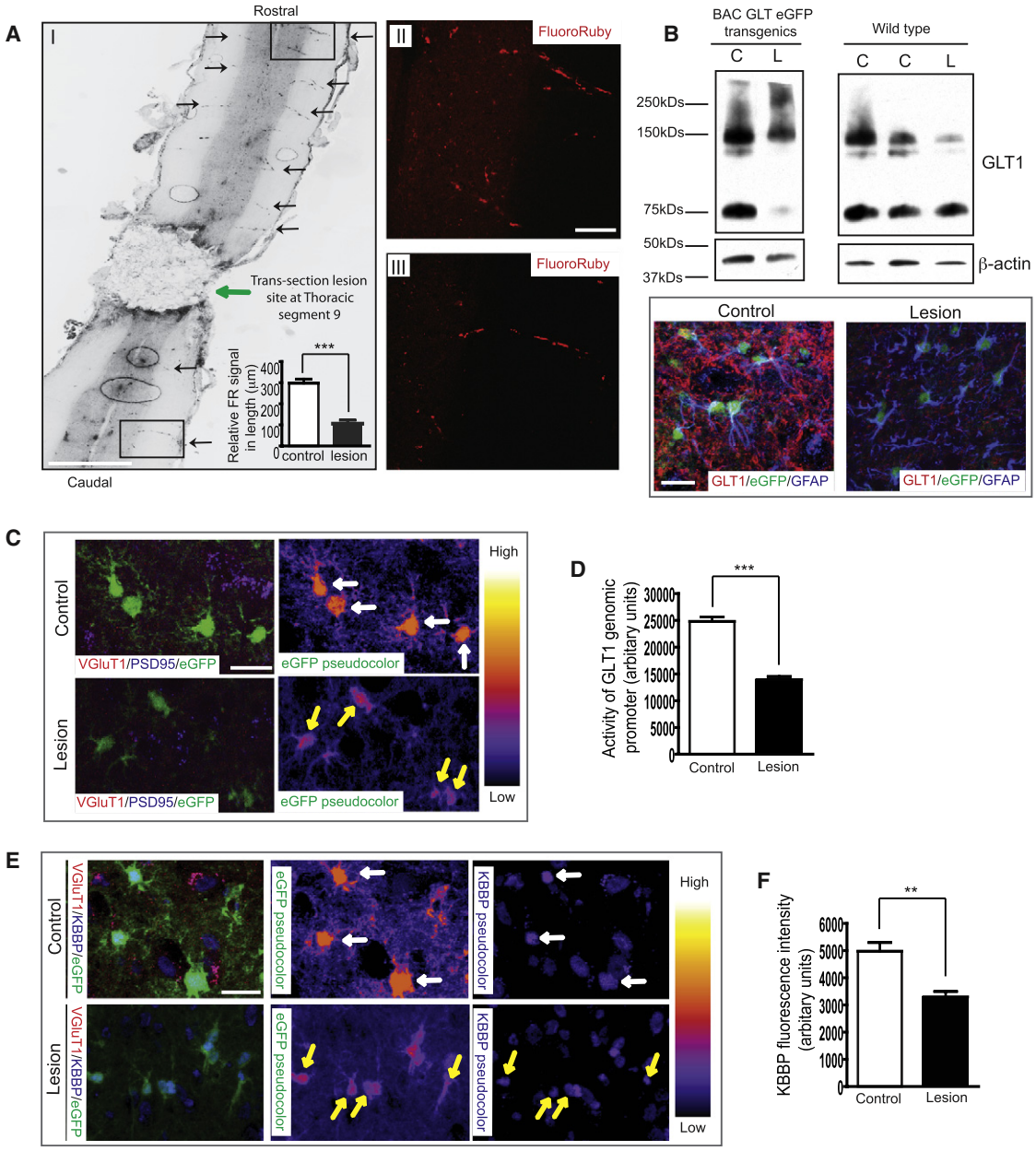

Figure 5. Corticospinal Tract Presynaptic Degeneration Induced by Spinal Cord Transection Results in Loss of GLT1 Protein and Promoter Activity

(A) Thoracic transection induces massive degeneration of descending axons. Descending corticospinal tracts were shown by anterograde transport of FR from motor cortex. Abundant FR labeled axons/neurons (black arrow) were observed in white/gray matter of spinal cord above the lesion site (I, scale bar, 0.5 mm). Quantitative analysis of FR-labeled axon length showed that 70% of axons degenerated in lesioned mice compared to sham control mice (n = 5). Representative images with FR labeled axons/neurons are shown in II and III, scale bar, 20 μm.

(B) Thoracic spinal cord transection leads to loss of GLT1 protein in lumbar spinal cord by both immunoblotting (n = 3) and immunostaining. Scale bar, 20 μm.

(C) Single astrocyte analysis in vivo revealed loss of GLT1 promoter activity in astrocytes surrounding degenerated axons/presynaptic terminals of lesioned BAC GLT1 eGFP mice. Presynaptic complexes were identified by double staining for presynaptic VGluT1 and postsynaptic PSD95. Scale bar, 20 μm.

(D) Quantitative analysis of the eGFP fluorescence intensity in lumbar cord astrocytes of lesioned mice ($n \geq 93$).

(E) Axon degeneration decreases KBBP immunostaining intensity in lumbar cord astrocytes of lesioned BAC GLT1 eGFP mice. Scale bar, 20 μm.

(F) Quantitative analysis of the KBBP immunostaining intensity in lumbar cord astrocytes of lesioned mice ($n \geq 45$) (***$p < 0.001$, mean ± SEM).

ricin injection also developed clear paralysis only in ricin side (Movie S1), suggesting that retrograde ricin indeed induced dramatic motor neuron degeneration. The focal, selective loss of motor neurons and their recurrent collaterals was apparent on surrounding astroglia-eGFP fluorescence intensity was 30% reduced in ricin lesion side compared to that of control side

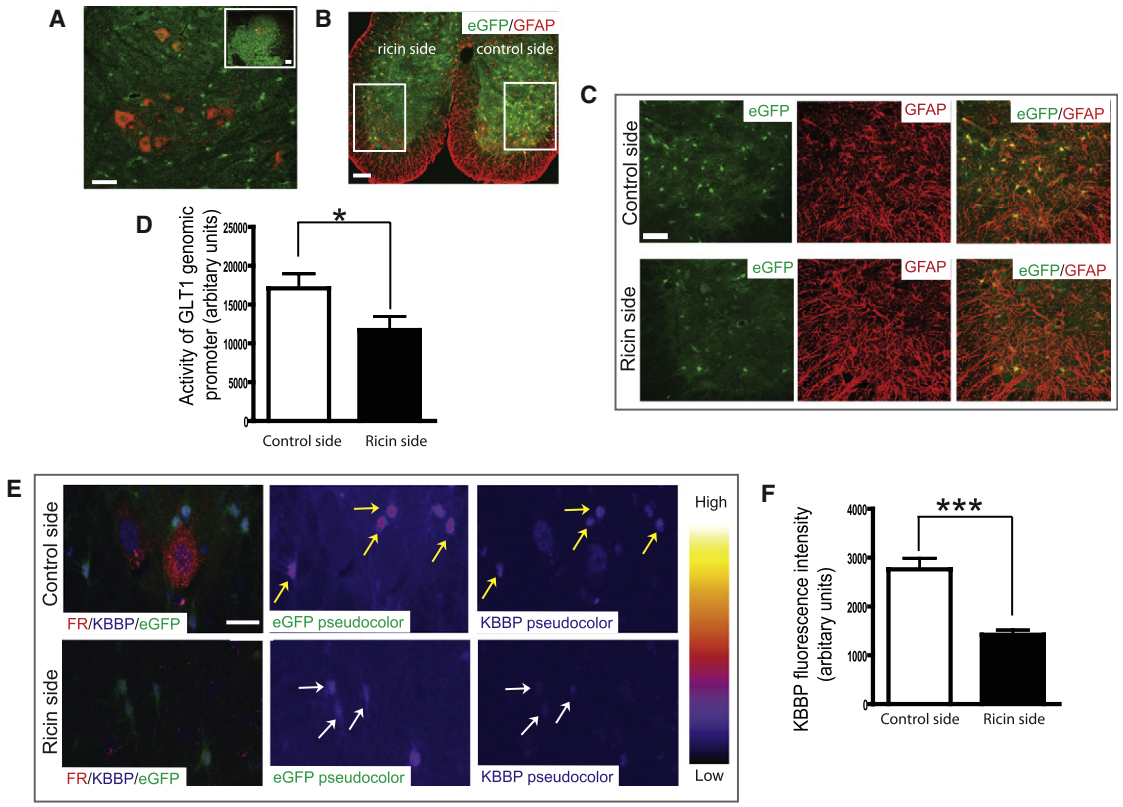

Figure 6. Motor Neuron Degeneration Induced by Neurotoxin Ricin Leads to Reduced GLT1 Promoter Activity and KBBP Expression

(A) Visualization of motor neurons in ventral horn of lumbar spinal cord by fluoro-ruby (FR). Femoral nerves were exposed and dipped into FR solution (10%) to allow retrograde transport of FR into motor neurons. Scale bar, 50 μm (insert scale bar, 100 μm).

(B) Unilateral administration of ricin induced reduction of eGFP intensity.

(C) Thin coronal sections of L2–L4 cord of BAC GLT1 eGFP mice was prepared and immunostained with GFAP antibody one week following unilateral administration of ricin. Reduced eGFP intensity but not the GFAP immunoreactivity was found in ricin side. Scale bar, 100 μm (50 μm for magnified image).

(D) Fluorescence intensity of eGFP in individual astroglial from ricin and control sides were measured in Image J and plotted using Prism (20–25 astrocytes per serial section/mouse for total 10 mice) (*$p < 0.05$, mean ± SEM, Student's t test).

(E) Single astrocyte analysis in vivo revealed reduction of KBBP immunoreactivity in astroglia with reduced eGFP intensity. Thin coronal sections of L2–L4 cord of BAC GLT1 eGFP mice was prepared and immunostained with KBBP antibody one week following unilateral administration of ricin. Motor neurons were identified by FR in control side.

(F) KBBP immunoreactivity in astroglia with reduced eGFP intensity was measured in Image J and plotted in Prism (20–25 astrocytes per serial section/mouse for total 10 mice). Scale bar, 20 μm. Yellow arrow: astroglia in control side; White arrow: astroglia in ricin side. (Student's t test: ***$p < 0.001$, mean ± SEM).

(Figures 6B, 6C, and 6D). This reduction of eGFP intensity was not due to astroglial death, as abundant GFAP immunoreactivity was still found in the astroglia with reduced eGFP on the lesioned side of the spinal cord (Figure 6C). Quantitative single astrocyte analysis of confocal images of thin section of L2-L4 cord from BAC GLT1 eGFP mice administrated with unilateral ricin also found 50% reduced KBBP immunoreactivity in astroglia with reduced eGFP intensity (Figures 6E and 6F). Ricin-induced motor neuron degeneration abolished its signaling to surrounding astroglia, likely mediated by both motor neuron dendrites and axon collaterals, which suggests that neuronal inputs are necessary to maintain KBBP expression levels and subsequent transactivation of the GLT1 promoter.

G93A SOD1 ALS Mouse Neurodegeneration

Severe loss of GLT1 protein has been observed in SOD1 G93A transgenic rodents (Howland et al., 2002), a model of familial ALS, and in the R6/2 mice model of Huntington's disease (Lievens et al., 2001). The mechanism for this loss in these animal models remains unexplained. Total spinal cord EAAT2 mRNA levels were not found abnormal in prior ALS studies (Bristol and Rothstein, 1996). However, these past studies were technically limited due to post mortem tissue artifacts and the use of low-resolution, bulk tissue homogenization and non-in situ approaches—all which limit the ability to detect focal astroglial abnormalities known to occur in human and rodent ALS (Howland et al., 2002; Rothstein et al., 1994a). Similar to the acute corticospinal lesion experiments and ricin toxin lesion, the loss of GLT1 protein in rodent models of ALS is focal to the region of degenerating motor neurons and spreads along the lumbar spinal cord. To better detect focal GLT1 mRNA alterations in astroglia, in situ hybridization of GLT1a and GLT1b, the two major GLT1 transcripts was performed in lumbar spinal cord of SOD1 G93A transgenic rat (Figure 7A). GLT1a mRNA is far more

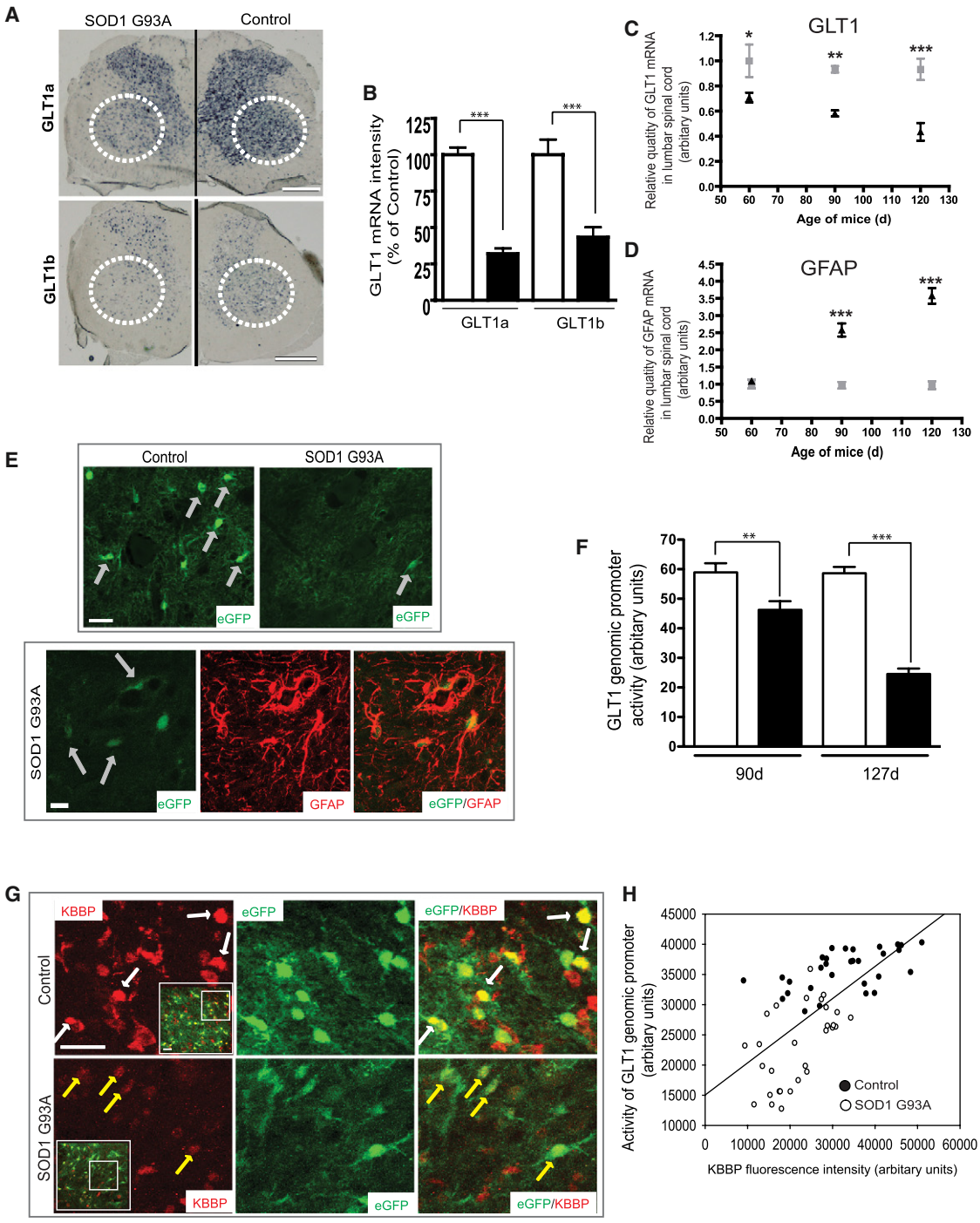

Figure 7. GLT1 Transcriptional Dysfunction Contributes to the Loss of GLT1 Protein in SOD1 G93A Rodents

(A) In situ hybridization of major GLT1 transcripts in lumbar cord of end-stage (125 days) SOD1 G93A rat. Scale bar, 0.5 mm.

(B) Quantitative analysis of in situ signals of GLT1a and GLT1b (20–30 areas examined per serial section per rat, n = 3 rats).

(C) QRT-PCR analysis of GLT1 mRNA levels in lumbar cord of SOD1 G93A mice.

(D) QRT-PCR analysis of GFAP mRNA levels in lumbar cord of SOD1 G93A mice. Total RNA from lumbar spinal cord of SOD1 G93A mice at different stages (60 days, 90 days, 120 days) was prepared. The GLT1 and GFAP mRNA levels were determined by QRT-PCR with GLT1- or GFAP-specific probe. The amount of RNA used in QRT-PCR was normalized by β-actin mRNA and 18 s RNA. The GLT1 or GFAP mRNA levels of WT mice at 60 days was used as calibrator for mRNA comparison (n = 7–12) (two-way ANOVA with post hoc Bonferroni: *$p < 0.05$, **$p < 0.01$, ***$p < 0.001$, mean ± SEM).

(E) Loss of GLT1 promoter activity indicated by eGFP intensity in astrocytes of ventral lumbar cord of BAC GLT1 eGFP X SOD1 G93A mice. No apparent loss of astroglia was observed by GFAP immunostaining.

abundant than GLT1b, which is consistent with previous studies (Berger et al., 2005). There was a pronounced focal loss of both GLT1a (70% loss compared to WT; Figure 7B) and GLT1b (50% loss compared to WT; Figure 7B) mRNA transcripts in the ventral horn of the SOD1 G93A rat spinal cord, similar to reports of GLT1 protein (Howland et al., 2002). In addition, quantitative real time PCR analysis of GLT1 mRNA from lumbar spinal cord of SOD1 G93A mice at different stage of disease progression (60, 90, 120 days) also showed that GLT1 mRNA was reduced to 65% of control at disease onset and further decreased to 40% of control as disease progressed to end stage (Figure 7C). In contrast, GFAP mRNA levels increased gradually as disease progressed to end stage (Figure 7D). To better evaluate alterations of GLT1 regulation at the single-cell level, the SOD1 G93A mice were mated to the GLT1 BAC eGFP reporter mice. The presence of the BAC-eGFP promoter reporter did not change the course of disease, with mice developing disease at approximately 90 days of age and reaching end stage at ~125 days of age (n = 20). BAC GLT1 eGFP × SOD1 G93A mice were sacrificed at various time points and eGFP expression, as a reflection of GLT1 promoter activity (Regan et al., 2007), was examined and quantified by confocal microscopy of serial thin sections from lumbar cord (Figure 7E). A profound decrease of astroglial GLT1 promoter activity, indicated by a more than 60% loss of eGFP fluorescence intensity, was found in ventral gray matter of BAC GLT1 eGFPxSOD1 G93A mice, especially in ventral gray matter-localized astroglia near motor neurons from end-stage (127 days) animals (Figure 7F). The loss of GLT1 promoter activity/eGFP fluorescence was the result of transcriptional dysfunction in these spinal cord astroglia, rather than cell death as increased GFAP immunostaining signal was observed from astrocytes with decreased eGFP fluorescence (Figure 7E), as well as increased GFAP mRNA levels in lumbar spinal cord from end-stage SOD1 G93A mice (Figure 7D). Notably, there is a profound loss of presynaptic terminals in this transgenic model as a result of the loss of presynaptic corticospinal tract terminals, spinal interneurons and recurrent collaterals from motor neurons, as reflected by a decrease in synaptophysin expression (Figure S4A; Morrison et al., 1998).

To determine if there was a relationship between neural injury/synaptic loss and the alteration in regulation of astroglial synaptic control in this disease model, the expression level of astroglial KBBP in ventral lumbar cord of BAC GLT1 eGFP × SOD1 G93A mice (n = 5) was also examined. As shown in Figure 7G, KBBP immunostaining and GLT1 promoter activity/eGFP reporter fluorescence was diminished in astrocytes from ventral lumbar cord of SOD1 G93A mice. The intensity of eGFP fluorescence and KBBP immunostaining in individual astrocytes ($n \geq 25$) were highly correlated (Figure 7H). Decreased KBBP expression levels (<20000, arbitrary units) were correlated with lower levels of eGFP fluorescence intensity (<25,000, arbitrary units), which was also found in the corticospinal transection and ricin models described above. GLT1 transcriptional activation, KBBP immunoreactivity and eGFP expression levels were unaltered in dorsal horn astrocytes from the BAC GLT1 eGFPxSOD1 G93A mice (data not shown).

In summary, KBBP is a *neuron-dependant* downstream nuclear factor that regulates astroglial GLT1 transcription as determined by (1) in vitro and in vivo genetic analysis of KBBP modulating GLT1 expression, (2) pharmacologic and synaptic activity regulated expression of GLT1 transcription, (3) correlation of developmental KBBP and GLT1 expression levels in astroglia, and (4) correlation of altered in vivo presynaptic inputs to astroglial KBBP and GLT1 promoter activation by employing models of synaptic denervation including corticospinal lesion, single neuron toxin lesion and an animal model of ALS. These studies provide a molecular mechanism for abnormal astroglia in neurodegeneration: alteration/loss of synaptic terminals decreases the astroglial expression of KBBP, which ultimately negatively regulates astroglial expression of the perisynaptic GLT1.

DISCUSSION

In this study, we systematically dissected the mechanisms underlying neuronal regulation of astroglia, by examining the neurotransmitter transporter EAAT2/GLT1 in complementary in vitro and in vivo models. Our results show that axonal interactions with astroglia are sufficient and necessary for neuron-dependent astroglial GLT1 transcriptional activation. Physiologically, presynaptic-based activation of astroglial GLT1 transcription could serve as a neuron-glial coupled mechanism ultimately for the modulation of postsynaptic activation at excitatory synapses, by regulating the synthesis of GLT1 and its subsequent expression on astroglial membranes. The current study identified a critical downstream astroglial nuclear factor KBBP and demonstrated that the recruitment of KBBP to the GLT1 promoter is required for neuron-dependent GLT1 transcriptional activation. Although prior studies, of cultured fetal astrocytes and small promoter fragments, suggested that NF-κB could modulate this promoter (Sitcheran et al., 2005; Su et al., 2003), physiologically relevant neuron-stimulated promoter activation was not dependent upon that transcription factor in the current study. Normal developmental maturation of new synapses correlated with the activation of astroglial GLT1, via new KBBP expression. The loss of presynaptic signaling to astrocytes, as a result of acute axon transection or neuronal death in an acute or chronic neurodegeneration model, abolished signal transmission from neurons to astroglia leading to transcriptional dysregulation: decreased astroglial KBBP, subsequent diminished GLT1 promoter activation and loss of GLT1 protein expression.

(F) Quantitative analysis of eGFP fluorescence intensity in astrocytes of BAC GLT1 eGFP X SOD1 G93A at different ages (35 astrocytes per serial section/mouse for total 20 mice).

(G) Decreased expression levels of KBBP in astrocytes with reduced eGFP fluorescence intensity in ventral lumbar cord of BAC GLT1 eGFP X SOD1 G93A mice. Scale bar, 20 μm (insert scale bar, 50 μm).

(H) Linear regression curve between KBBP immunoreactivity and eGFP intensity in astroglia. KBBP immunoreactivity and eGFP fluorescence intensity was measured in Image J and plotted in SigmaPlot. ($n \geq 25$) (Student's t test: ***$p < 0.001$, mean ± SEM).

Axon induced GLT1 activation is likely to be mediated by both presynaptic secretion and membrane contact. Previous in vitro preparations of simple mixed neuron-glial cultures had suggested that neuron secreted factors could activate astroglial differentiation and expression of GLT1 (or GLAST) (Gegelashvili et al., 1997; Munir et al., 2000; Schlag et al., 1998). The elements responsible for this neuron-glial interaction, e.g., dendrites, axons, synapses, receptor subtypes, are not known. In the current study, using the microfluidic culture platform, we were able to identify axon/presynaptic inputs as a distinct regulator of astroglial transporter activation, via KBBP. In parallel, we also identified comparable presynaptic inputs as a necessary component of KBBP activation of astroglial GLT1 in vivo. The mechanism of GLT1 regulation appears to involve both glutamate receptors as well as unspecified membrane-membrane interactions. For example, axon-glial membrane contact can be a potent regulator of developmental astroglial Notch signaling (Eiraku et al., 2005). In addition, neurons may also modulate the nontranscriptional processes in astrocyte-specific synaptic functions such as trafficking and membrane stabilization or clustering of GLT1 protein as suggested by in vitro studies (Nakagawa et al., 2008; Zhou and Sutherland, 2004).

Downstream signaling pathways between GluRs and KBBP recruitment to the GLT1 promoter are not yet understood. As KBBP can be phosphorylated by multiple upstream protein kinases (Bomsztyk et al., 2004), signals may be transmitted from GluRs to KBBP by protein kinase mediated phosphorylation. KBBP likely acts as a docking platform to aid in actions of other transcription factors with the GLT1 promoter. The interaction of KBBP with other astroglia-specific transcription factors remains to be characterized.

Expression of neurodegenerative disease proteins, including mutant SOD1, Huntington's disease protein, and spinocerebellar ataxia 7 protein—have all implicated astroglial dysfunction in disease propagation (Lobsiger and Cleveland, 2007) with unclear mechanisms why astroglia becomes dysfunctional in diseases. Although multiple mechanisms likely contribute to motor- and interneuron death in ALS and its familial transgenic models, astroglial loss of GLT1/EAAT2 in both sporadic and familial ALS represents a common mechanism for disease propagation. Notably, a high percentage ($\geq$50%) of motor/inter neuron degeneration has occurred at the time when symptoms start to develop (Martin et al., 2007), which is consistent with the loss of synaptophysin we observed. Synaptic stripping and loss of presynaptic inputs to neurons are described in animal models of neurodegeneration/neural injury (Blinzinger and Kreutzberg, 1968; Trapp et al., 2007) and in humans (Graeber et al., 1993). Our current studies suggest that disruption of the neuron-astroglial unit, specifically the loss of synaptic terminals/synaptic activity, alters normal astroglial function. It is likely that changes in synaptic terminals induce astroglial dysfunction—such as altered GLT1 expression and other synaptically relevant proteins which leads to additional neuronal injury and thereby acts as a feed forward mechanism to propagate neuronal disease/injury. A more complete understanding of the global transcriptional changes in astrocytes following neuronal injury may help identify other pathways by which astroglia contribute to normal and abnormal brain function.

EXPERIMENTAL PROCEDURES

Cultures and Transfection

Cortical astrocyte cultures were prepared from P2–4 mouse pups. Cortical neuronal cultures were prepared from E14–16 mouse embryos. For astrocyte-neuron coculture on the MCP, chambers were first assembled on coated glass-bottom dishes before culturing as previously described (Park et al., 2006). Neuronal cultures (>1 × 10^6 cells) were directly seeded on the right side of the MCP (N in Figure 1A) and GDNF (10 ng/ml) was applied to the left side for 3–5 days to induce axon outgrowth. GDNF was removed and astrocytes (precultured for 7-10d) were then plated on the left side of the MCP (before axons grow through the channels) for another 3–5 days. Electroporation of astrocyte cultures with promoter reporter and shRNA constructs was performed by using an Amaxa device (Gaithersburg, MD). In each reaction, 2–4 × 10^6 cells and 4 μg DNA was used. Organotypic spinal cord slice cultures were prepared and treated as described previously (Rothstein et al., 1993).

Immunostaining and Microscopy

Cultures were directly fixed in the MCP with 4% paraformaldehyde (30 min). After three rinses in PBS, cells were treated with blocking buffer (0.4% BSA, 5% goat-serum, and 0.2% Triton X-100 in PBS) for 20 min at room temperature. Primary antibodies GLT1 (rabbit, 1:1000), βIII-tubulin (mouse, 1:1000), Synaptin I (rabbit, 1:1000), 2G13 (mouse, 1:50) were incubated overnight at 4°C in blocking buffer. Anti-mouse Alexa 488-conjugated antibody or anti-rabbit Alexa 555-conjugated antibody (1:1000) were added for 90 min at room temperature. For immunohistochemistry, animals were perfused with 4% paraformaldehyde. Tissues were dissected and kept in 4% paraformaldehyde overnight. After PBS wash, tissues were cryoprotected in 30% sucrose overnight and embedded in tissue freezing medium. Except for spinal cord from transection lesioned mice (15 μm horizontal section), serial coronal sections (30 μm for brain and 15 μm for spinal cord) were prepared. Sections were incubated in blocking buffer (Tris-Cl [pH 7.4], 5% goat serum, 0.1% Triton X-100, 1% BSA) for 60 min. Primary antibodies KBBP (1:1000), GLT1 (1:500), GFAP (1:200), VGluT1 (1:200), PSD95 (1:200) were incubated overnight at 4°C in blocking buffer. Anti-mouse/rabbit Alexa 555-conjugated antibody or anti-mouse/rabbit Alexa 633-conjugated antibody (1:1000) were added for 90 min at room temperature. All double staining was performed sequentially. Confocal images of stained MCP or tissue sections were taken on Zeiss LSM510 Meta. For live-cell time-lapse imaging on the MCP, astrocytes from BAC GLT1 eGFP mice were used. Images were taken from 24 to 112 hr post-seeding of astrocytes. Images were taken simultaneously on both green and transmitted filter. eGFP fluorescence intensity was digitally converted into a rainbow pseudocolor (Image J).

Plasmids and Virus Preparation

Fragments of GLT1/EAAT2 promoter sequence was amplified with pfu and cloned into XhoI/HindIII site of pGL4.14 vector to generate luciferase promoter reporters. Individual sites on the GLT1/EAAT2 promoter were mutagenized by gene tailor system (Invitrogen, Carlsbad, CA) and cloned into pGL4.14. GLT1/EAAT2 promoter DsRed reporter was generated by inserting GLT1/EAAT2 promoter fragment into XhoI/HindIII site of pDsRed-Express-1. GLT1/EAAT2 promoter fragment and DsRed cassette were prepared by XhoI/XbaI digestion and then cloned into modified pAM/CAG-pL-WPREBGH-polyA viral vector for final AAV construct. KBBP and NS (nonspecific) small hairpin RNA (shRNA) was synthesized and cloned into pGSU6-GFP to test its efficiency. KBBP and luciferase antisense was reversely amplified from pGK5 and pGL4.14 by pfu and cloned into XhoI/EcoRI site of pAM-pGFA-pL-WPREBGH-polyA. For overexpression constructs of KBBP and luciferase, KBBP and luciferase cDNA was subcloned into the EcoRI/XhoI site of pcDNA 3.1/myc-His vector. Recombinant AAV8 was packaged in cultures of HEK293T cells. Adeno helper plasmid (pFD6), AAV helper encoding serotype 8 (pAR8), and the AAV transgene vector plasmid were transfected into HEK293T cells using polyfect (QIAGEN, Valencia, CA). At 72 hr after transfection, cells were pelleted by centrifugation and resuspended in 10 mM Tris-cl (pH 8.0). AAV8 viral particles were purified by density gradient centrifugation (60,000 rpm, 2 hr) in iodixinol after lysing cells, followed by centrifugation in Millipore Ultrafree 15 filter

devices. The titer of virus (genomic particles/ml) was determined by quantitative RT-PCR using primers and a probe specific for the WPRE sequence.

Quantitative RT-PCR

Total RNA from either cultured cells or tissues were prepared by using Absolutely RNA Miniprep Kit from Stratagene. Total RNA were converted to cDNA and TaqMan premade gene-specific probes for were used for PCR process. 18 s rRNA was used as endogenous marker to normalize the RNA quantity.

Gel Shift and Affinity Purification

Wild-type and mutant oligos (45-mer) from −707 to −663 of EAAT2 promoter were directly synthesized with biotin added to the 5′ end. Mutant oligos have sequence from −688 to −679 GGGTGGGTGT replaced with AAATGCCACT. Nuclear extracts were prepared by using NE-PER Nuclear and Cytoplasmic Extraction Reagent (Pierce Biotechnology, Rockford, IL) from freshly dissected cortex of P2 and P21 wild-type mice. Gel shift was performed with procedures described in Lightshift Chemiluminescent EMSA kit (Pierce Biotechnology, Rockford, IL). In each reaction, 2 μl (50 fmol/μl) biotin labeled oligos with 100-fold unlabeled oligo, and 5 μg nuclear extract were added. The same oligos and nuclear extracts from P21 mice cortex were used for affinity purification. Affinity purification was performed using a μMACS FactorFinder kit (Milteny Biotec, Auburn, CA). For each reaction, 50 μg of nuclear extracts and 10 μl (5 pmol/μl) biotin labeled oligos were mixed and two reactions were pooled together for WT or mutant oligos, respectively. Elutions were resolved on 4%–12% gradient gel and stained by using SilverSNAP Stain for Mass Spectrometry (Pierce Biotechnology, Rockford, IL). Silver stained bands were excised and digested by trypsin, and subjected to LC/MS/MS analysis at Johns Hopkins University Mass Spectrometry Facility (Baltimore, MD).

In Situ Hybridization

Lumbar spinal cords (L4–5) were carefully dissected from end-stage (135 days) SOD1 G93A and age-matched control rats and snap-frozen into −80°C. Coronal sections (10 μm) of lumbar cord were prepared. Specific 3′UTR cRNA probes (400 bp) for GLT1a and GLT1b were amplified from mouse genomic DNA and in vitro transcribed, respectively. The exact location of GLT1a and GLT1b were previously described (Berger et al., 2005; Rothstein et al., 1994b). Single-label nonisotopic in situ hybridization was performed with digoxigenin (DIG)-labeled cRNA probes and alkaline phosphatase (AP) detection as described previously (Rothstein et al., 1996).

Animals, Virus Injection, and Surgery

Wild-type Sprague-Dawley rats and C57/B6 mice, SOD1 G93A transgenic rats and mice, BAC GLT1 eGFP transgenic mice were used for in vivo experiments. The care and treatment of animals in all procedures strictly followed the NIH Guide for the Care and Use of Laboratory Animals and the Guidelines for the Use of Animals in Neuroscience Research and the Johns Hopkins University IACUC. Rats and mice were housed at standard temperature (21°C) and in a light controlled environment with ad libitum access to the food and water. BAC GLT1 eGFP reporter mice were crossed with SOD1 G93A mice to obtain double-transgenic mice. Littermates were used as control. BAC GLT1 eGFP transgenic mice were made as previously described (Regan et al., 2007). For AAV8 injection, 2.5 μl virus ($10^{12–13}$ genome particle/ml) particles mixed with 0.5 μl 0.2% fast green was injected by glass capillary micropipette into cerebral lateral ventricle of P0 pups of BAC GLT1 eGFP transgenic mice. Mice were sacrificed three weeks after injection. For thoracic transection and ricin administration, mice (8 weeks old) received i.p. injections of anesthetic cocktail (ketamine [95 mg/kg; Fort Dodge Animal Health; Fort Dodge, IA] and xylazine [10 mg/kg; Bayer, Shawnee Mission, KS]). After anesthesia, a laminectomy was performed above the T9 spinal cord level and the dura was excised above the injury site using a 30-gauge needle. Microscissor cuts were made at both the rostral and caudal extents of the T9 spinal cord level to remove the T9 segment, followed by gentle aspiration in the lesion cavity. A small piece of Gelfoam was used to fill the lesion cavity. Postoperative care included buprenorphine (Reckitt Benckiser; Richmond, VA), subcutaneous injection of lactated ringers' solution and twice-daily expression of bladders up to 7 days postinjury. For Ricin administration, femoral nerves on both sides were exposed and transected. The nerves were then crushed about 15 mm proximal to transection and dipped into fluoro-ruby (FR, 10%) or mixture of ricin (final concentration, 1 mg/ml) and FR(10%) solution for 60 min.

Image Quantification, Graphics, and Statistical Analysis

All quantitative analysis of images was performed in Image J by measuring the intensity of signals. Data was plotted in PRISM (GraphPad Software, Inc) or SigmaPlot (SPSS). Two-way and one-way ANOVA (Bonferroni post hoc analysis) along with Student's t test were used for statistical analysis where appropriate (details, see figure legends) (JMP software, ver.7; SAS Inst. Cary, NC). p values < 0.05 were considered significant employing a two-tailed analysis. In some cases, quantification of gels was performed by Quantity One Software (BioRad Inc. Hercules, CA).

SUPPLEMENTAL DATA

The Supplemental Data include six figures and one movie and can be found with this article online at http://www.neuron.org/supplemental/S0896-6273(09)00155-X.

ACKNOWLEDGMENTS

This work was supported by NIH: NS33958 (J.D.R.), NS36465 (M.B.R., J.D.R.); the Robert Packard Center for ALS Research; Muscular Dystrophy Association (Y.Y.).

Accepted: February 17, 2009
Published: March 25, 2009

REFERENCES

Arnth-Jensen, N., Jabaudon, D., and Scanziani, M. (2002). Cooperation between independent hippocampal synapses is controlled by glutamate uptake. Nat. Neurosci. *5*, 325–331.

Berger, U.V., DeSilva, T.M., Chen, W., and Rosenberg, P.A. (2005). Cellular and subcellular mRNA localization of glutamate transporter isoforms GLT1a and GLT1b in rat brain by in situ hybridization. J. Comp. Neurol. *492*, 78–89.

Blinzinger, K., and Kreutzberg, G. (1968). Displacement of synaptic terminals from regenerating motoneurons by microglial cells. Z. Zellforsch. Mikrosk. Anat. *85*, 145–157.

Bomsztyk, K., Denisenko, O., and Ostrowski, J. (2004). hnRNP K: one protein multiple processes. Bioessays *26*, 629–638.

Bristol, L.A., and Rothstein, J.D. (1996). Glutamate transporter gene expression in amyotrophic lateral sclerosis motor cortex. Ann. Neurol. *39*, 676–679.

Broekman, M.L., Comer, L.A., Hyman, B.T., and Sena-Esteves, M. (2006). Adeno-associated virus vectors serotyped with AAV8 capsid are more efficient than AAV-1 or −2 serotypes for widespread gene delivery to the neonatal mouse brain. Neuroscience *138*, 501–510.

Chaudhry, F.A., Lehre, K.P., van Lookeren, C.M., Ottersen, O.P., Danbolt, N.C., and Storm-Mathisen, J. (1995). Glutamate transporters in glial plasma membranes: highly differentiated localizations revealed by quantitative ultrastructural immunocytochemistry. Neuron *15*, 711–720.

Danbolt, N.C. (2001). Glutamate uptake. Prog. Neurobiol. *65*, 1–105.

Eiraku, M., Tohgo, A., Ono, K., Kaneko, M., Fujishima, K., Hirano, T., and Kengaku, M. (2005). DNER acts as a neuron-specific Notch ligand during Bergmann glial development. Nat. Neurosci. *8*, 873–880.

Furuta, A., Rothstein, J.D., and Martin, L.J. (1997). Glutamate transporter protein subtypes are expressed differentially during rat CNS development. J. Neurosci. *17*, 8363–8375.

Gegelashvili, G., Danbolt, N.C., and Schousboe, A. (1997). Neuronal soluble factors differentially regulate the expression of the GLT1 and GLAST glutamate transporters in cultured astroglia. J. Neurochem. *69*, 2612–2615.

Genoud, C., Quairiaux, C., Steiner, P., Hirling, H., Welker, E., and Knott, G.W. (2006). Plasticity of astrocytic coverage and glutamate transporter expression in adult mouse cortex. PLoS Biol. *4*, e343. 10.1371/journal.pbio.0040343.

Graeber, M.B., Bise, K., and Mehraein, P. (1993). Synaptic stripping in the human facial nucleus. Acta Neuropathol. *86*, 179–181.

Halassa, M.M., Fellin, T., and Haydon, P.G. (2007). The tripartite synapse: roles for gliotransmission in health and disease. Trends Mol. Med. *13*, 54–63.

Howland, D.S., Liu, J., She, Y., Goad, B., Maragakis, N.J., Kim, B., Erickson, J., Kulik, J., DeVito, L., Psaltis, G., et al. (2002). Focal loss of the glutamate transporter EAAT2 in a transgenic rat model of SOD1 mutant-mediated amyotrophic lateral sclerosis (ALS). Proc. Natl. Acad. Sci. USA *99*, 1604–1609.

Huang, Y.H., and Bergles, D.E. (2004). Glutamate transporters bring competition to the synapse. Curr. Opin. Neurobiol. *14*, 346–352.

Lauriat, T.L., Richler, E., and McInnes, L.A. (2007). A quantitative regional expression profile of EAAT2 known and novel splice variants reopens the question of aberrant EAAT2 splicing in disease. Neurochem. Int. *50*, 271–280.

Lievens, J.C., Woodman, B., Mahal, A., Spasic-Boscovic, O., Samuel, D., Kerkerian-Le Goff, L., and Bates, G.P. (2001). Impaired glutamate uptake in the R6 Huntington's disease transgenic mice. Neurobiol. Dis. *8*, 807–821.

Lobsiger, C.S., and Cleveland, D.W. (2007). Glial cells as intrinsic components of noncell-autonomous neurodegenerative disease. Nat. Neurosci. *10*, 1355–1360.

Martin, L.J., Liu, Z., Chen, K., Price, A.C., Pan, Y., Swaby, J.A., and Golden, W.C. (2007). Motor neuron degeneration in amyotrophic lateral sclerosis mutant superoxide dismutase-1 transgenic mice: mechanisms of mitochondriopathy and cell death. J. Comp. Neurol. *500*, 20–46.

Morrison, B.M., Janssen, W.G., Gordon, J.W., and Morrison, J.H. (1998). Time course of neuropathology in the spinal cord of G86R superoxide dismutase transgenic mice. J. Comp. Neurol. *391*, 64–77.

Moumen, A., Masterson, P., O'Connor, M.J., and Jackson, S.P. (2005). hnRNP K: an HDM2 target and transcriptional coactivator of p53 in response to DNA damage. Cell *123*, 1065–1078.

Munir, M., Correale, D.M., and Robinson, M.B. (2000). Substrate-induced up-regulation of Na(+)-dependent glutamate transport activity. Neurochem. Int. *37*, 147–162.

Nakagawa, T., Otsubo, Y., Yatani, Y., Shirakawa, H., and Kaneko, S. (2008). Mechanisms of substrate transport-induced clustering of a glial glutamate transporter GLT-1 in astroglial-neuronal cultures. Eur. J. Neurosci. *28*, 1719–1730.

Ostrowski, J., Van Seuningen, I., Seger, R., Rauch, C.T., Sleath, P.R., McMullen, B.A., and Bomsztyk, K. (1994). Purification, cloning, and expression of a murine phosphoprotein that binds the kappa B motif in vitro identifies it as the homolog of the human heterogeneous nuclear ribonucleoprotein K protein. Description of a novel DNA-dependent phosphorylation process. J. Biol. Chem. *269*, 17626–17634.

Park, J.W., Vahidi, B., Taylor, A.M., Rhee, S.W., and Jeon, N.L. (2006). Microfluidic culture platform for neuroscience research. Nat. Protoc. *1*, 2128–2136.

Regan, M.R., Huang, Y.H., Kim, Y.S., Dykes-Hoberg, M.I., Jin, L., Watkins, A.M., Bergles, D.E., and Rothstein, J.D. (2007). Variations in promoter activity reveal a differential expression and physiology of glutamate transporters by glia in the developing and mature CNS. J. Neurosci. *27*, 6607–6619.

Rothstein, J.D., Martin, L.J., and Kuncl, R.W. (1992). Decreased glutamate transport by the brain and spinal cord in amyotrophic lateral sclerosis. N. Engl. J. Med. *326*, 1464–1468.

Rothstein, J.D., Jin, L., Dykes-Hoberg, M., and Kuncl, R.W. (1993). Chronic inhibition of glutamate uptake produces a model of slow neurotoxicity. Proc. Natl. Acad. Sci. USA *90*, 6591–6595.

Rothstein, J.D., Martin, L., Dykes-Hoberg, M., Jin, L., Levey, A., and Kuncl, R.W. (1994a). Glutamate transporter subtypes: role in excitotoxicity and amyotrophic lateral sclerosis. Ann. Neurol. *36*, 282.

Rothstein, J.D., Martin, L., Levey, A.I., Dykes-Hoberg, M., Jin, L., Wu, D., Nash, N., and Kuncl, R.W. (1994b). Localization of neuronal and glial glutamate transporters. Neuron *13*, 713–725.

Rothstein, J.D., Dykes-Hoberg, M., Pardo, C.A., Bristol, L.A., Jin, L., Kuncl, R.W., Kanai, Y., Hediger, M.A., Wang, Y., Schielke, J.P., and Welty, D.F. (1996). Knockout of glutamate transporters reveals a major role for astroglial transport in excitotoxicity and clearance of glutamate. Neuron *16*, 675–686.

Rothstein, J.D., Patel, S., Regan, M.R., Haenggeli, C., Huang, Y.H., Bergles, D.E., Jin, L., Dykes Hoberg, M., Vidensky, S., Chung, D.S., et al. (2005). Beta-lactam antibiotics offer neuroprotection by increasing glutamate transporter expression. Nature *433*, 73–77.

Schlag, B.D., Vondrasek, J.R., Munir, M., Kalandadze, A., Zelenaia, O.A., Rothstein, J.D., and Robinson, M.B. (1998). Regulation of the glial Na+-dependent glutamate transporters by cyclic AMP analogs and neurons. Mol. Pharmacol. *53*, 355–369.

Schmitt, A., Asan, E., Puschel, B., Jons, T., and Kugler, P. (1996). Expression of the glutamate transporter GLT1 in neural cells of the rat central nervous system: nonradioactive in situ hybridization and comparative immunocytochemistry. Neuroscience *71*, 989–1004.

Sitcheran, R., Gupta, P., Fisher, P.B., and Baldwin, A.S. (2005). Positive and negative regulation of EAAT2 by NF-kappaB: a role for N-myc in TNFalpha-controlled repression. EMBO J. *24*, 510–520.

Su, Z.Z., Leszczyniecka, M., Kang, D.C., Sarkar, D., Chao, W., Volsky, D.J., and Fisher, P.B. (2003). Insights into glutamate transport regulation in human astrocytes: cloning of the promoter for excitatory amino acid transporter 2 (EAAT2). Proc. Natl. Acad. Sci. USA *100*, 1955–1960.

Sutherland, M.L., Delaney, T.A., and Noebels, J.L. (1996). Glutamate transporter mRNA expression in proliferative zones of the developing and adult murine CNS. J. Neurosci. *16*, 2191–2207.

Swanson, R.A., Liu, J., Miller, J.W., Rothstein, J.D., Farrell, K., Stein, B.A., and Longuemare, M.C. (1997). Neuronal regulation of glutamate transporter subtype expression in astrocytes. J. Neurosci. *17*, 932–940.

Tanaka, K. (1997). Epilepsy and exacerbation of brain injury in mice lacking glutamate transporter GLT-1. Science *276*, 1699–1702.

Trapp, B.D., Wujek, J.R., Criste, G.A., Jalabi, W., Yin, X., Kidd, G.J., Stohlman, S., and Ransohoff, R. (2007). Evidence for synaptic stripping by cortical microglia. Glia *55*, 360–368.

Zelenaia, O., Schlag, B.D., Gochenauer, G.E., Ganel, R., Song, W., Beesley, J.S., Grinspan, J.B., Rothstein, J.D., and Robinson, M.B. (2000). Epidermal growth factor receptor agonists increase expression of glutamate transporter GLT-1 in astrocytes through pathways dependent on phosphatidylinositol 3-kinase and transcription factor NF-kappaB. Mol. Pharmacol. *57*, 667–678.

Zhou, J., and Sutherland, M.L. (2004). Glutamate transporter cluster formation in astrocytic processes regulates glutamate uptake activity. J. Neurosci. *24*, 6301–6306.